REPORT DOCUMENTATION PAGE

AFRL-SR-BL-TR-00-

0650

1. AGENCY USE ONLY (Leave blank)	2. REPORT DATE	3. REPORT TYPE AND DATES COVERED
	1 October 2000	Final Technical, 1 August 1997 - 30 June 2000

4. TITLE AND SUBTITLE

NWV Topic 20 Jam-Proof Area Deniable Propagation: Anti-Jam Protection for GPS via Robust Efficient Space-Time Adaptive Processing

5. FUNDING NUMBERS

F49620-97-1-0275

6. AUTHOR(S)

Dr. Michael D. Zoltowski

7. PERFORMING ORGANIZATION NAME(S) AND ADDRESS(ES)

Purdue University, W. Lafayette, IN 47907

8. PERFORMING ORGANIZATION REPORT NUMBER

Purdue TR-EE-00-7

9. SPONSORING / MONITORING AGENCY NAME(S) AND ADDRESS(ES)

Air Force Office of Scientific Research
801 North Randolph Street Room 732
Arlington VA 22203-1977

10. SPONSORING / MONITORING AGENCY REPORT NUMBER

11. SUPPLEMENTARY NOTES

12a. DISTRIBUTION / AVAILABILITY STATEMENT

Distribution Unlimited

12b. DISTRIBUTION CODE

13. ABSTRACT *(Maximum 200 Words)*

This effort focused on the development of algorithms and systems for protecting military Global Positioning Satellite (GPS) receivers from being jammed. Several very promising signal processing algorithms have been developed that provide a high degree of anti-jam (AJ) protection. An innovative space-time preprocessor was developed based on the multistage nested Wiener filter of Goldstein and Reed. Insight was developed into the dependency of the Wiener-Hopf filter weights on the number of stages and the blocking matrices employed at each stage. The preprocessor was shown to rapidly null out both narrowband and wideband jammers while operating in a reduced-rank mode and minimizing computational complexity. Smoothing measures were incorporated into the AJ algorithms to minimize any distortion induced on the GPS signals themselves in the process of canceling the jammers. As listed in Section 6, this research has been extensively published in journals and presented at a number of high-profile conferences on signal processing and communications. Transitions of this research to Wright Laboratories at Wright-Patterson Air Force base, Rome Labs, and Eglin Air Force Base are in progress.

14. SUBJECT TERMS	15. NUMBER OF PAGES
GPS, smart antennas, anti-jam spatial filter, space-time processing, adaptive beamforming	26
	16. PRICE CODE

17. SECURITY CLASSIFICATION OF REPORT	18. SECURITY CLASSIFICATION OF THIS PAGE	19. SECURITY CLASSIFICATION OF ABSTRACT	20. LIMITATION OF ABSTRACT
UNCLASSIFIED	UNCLASSIFIED	UNCLASSIFIED	UL

New World Vista Topic 20:
Jam-Proof Area Deniable Propagation: Anti-Jam Protection for GPS Via Robust, Computationally Efficient Space-Time Adaptive Processing

FINAL TECHNICAL REPORT

Air Force Office of Scientific Research

Grant/Contract Number: F49620-97-1-0275

Period Covered: 1 August 1997 - 30 June 2000

Principal Investigator:

Michael D. Zoltowski

School of Electrical Engineering
1285 Electrical Engineering Building
Purdue University
West Lafayette, IN 47907 USA
e-mail: mikedz@ecn.purdue.edu
Phone: 765-494-3512
FAX: 765-494-0880

Program Director:

Dr. Jon A. Sjogren

AFOSR/NM
801 North Randolph Street Room 732
Ballston Towers
Arlington VA 22203-1977
jon.sjogren@afosr.af.mil
Phone: 703-696-6564
FAX: 703-696-8450

1 ACCOMPLISHMENTS: EXECUTIVE SUMMARY OF RESEARCH

1.1 Technical Objective and Expected Payoff

The enemy threat to GPS is evolving in two areas: enemy use of GPS and the enemy's ability to deny GPS to the United States. Worldwide military use of GPS is evolving due to the wide availability of commercial GPS receivers, and the widespread knowledge of the force enhancement capabilities offered by GPS. The jamming threat is a concern because of the physical design of the GPS system. The received power from the GPS satellites is approximately -157 dBW. Many jammers available on the arms market today either already cover the GPS frequencies, or can be modified to do so.

The technical objective is to identify, evaluate, develop, and demonstrate innovative anti-jam (AJ) processors that are effective against intentional and unintentional interference to GPS user equipment. This entailed a system-level study of the trade-offs between protection performance versus hardware and computational complexity for various integrated levels of processing. *The primary end objective is the development of fully digital AJ solutions that are integrated into the GPS receiver to achieve higher, yet affordable AJ capabilities for GPS user equipment on navy cruisers, aircraft, and airborne weapons systems.* However, AJ preprocessors which may be implemented as retro-fits to either existing or currently planned GPS receivers have been developed as well.

The expected payoff arises from the proven ability of GPS to provide significant force enhancement capability. This force enhancement capability has been demonstrated in every U.S. military operation since and including the Gulf War. The success of GPS in these operations has led to an increasing Department of Defense (DoD) and Allied reliance on GPS. To date, over 200,000 GPS receivers have been delivered to the DoD and its Allies. GPS uses include navigation targeting, sensor aiding, weapons delivery, timing, and battlefield command/control. *A key performance feature of the algorithms that have been developed is the ability to defeat electronic attack, including the smart or spoofing jammer.*

The time is right for a fully digital solution so that the expected pay-off should be very substantial. From a signalling viewpoint, GPS is a Code Division Multiple Access (CDMA) system wherein each satellite is assigned a different code. The Third Generation (3G) of *commercial* cellular CDMA systems is currently under development. To support wireless access to the Internet, for the downloading of video in real-time, for example, it is planned that 3G CDMA systems will accommodate bandwidths up to 20 MHz -- same as the bandwidth occupied by the P code signal! Texas Instruments (TI) and other companies are now producing DSP chips that do CDMA processing commensurate with this bandwidth. In addition, commercial CDMA systems involve correlations with a so-called "long" code that is similar in nature (roughly speaking) to the P code. Further, part of 3G CDMA will operate in a band centered at 1.9 GHz, not very far in frequency from L1.

The point is that in the very near future fully digital solutions effecting AJ for GPS may be feasibly implemented on commercially available DSP chips developed for 3G CDMA.[1] These DSP chips will be mass produced facilitating a cost effective solution.

The overall goal of this project is to develop an affordable GPS system-level solution that protects DoD's and U.S. Allies' continuous operational use of GPS.

2 Military Problem/Deficiency Addressed and Resulting Capability Enhancements

2.1 Deficiency Addressed

The success of GPS in Desert Storm and other operations has increased DoD's commitment to equipping weapon systems with GPS receivers. However, this commitment has been accompanied by a

[1] It is interesting to note that just as GPS chip sets are coming down in price enough to be feasible for use in cell phones for 911 Emergency Geolocation, the DSP chips embedded in cell phones are becoming advanced enough to process signals at the P code rate.

heightened awareness of the potential vulnerabilities of GPS to both intentional and unintentional RF interference. Limited Electronic Counter Counter Measures have been developed over the past two decades primarily based on the null steering Controlled Reception Pattern Antenna (CRPA) and associated Antenna Electronics (AE). However, this spatial filter technology is limited in its ability to cancel jammers due to component, device, and technology limitations, as well as the increasing potential jamming threat.

For example, the CRPA AE system was one of the earliest anti-jam spatial filters for GPS, a seven element null steering antenna array. The principle used in the CRPA AE system (deployed on F-16C fighters) to cancel interference is power minimization. Power minimization is premised on the fact that prior to correlation, the C/A code signal from any one GPS satellite is on the order of 30 dB below the noise floor. In power minimization based null steering, the weight for the reference antenna is set to unity and the remaining weights applied to the auxiliary antennas are found as those which drive the output power of the beamformer as close to the noise floor as possible. This adaptively steers nulls in the directions of those interferers whose power levels are above the noise floor.

The CRPA AE system employed vector modulators to effect the weights applied to the auxiliary antennas at RF. Vector modulators are digitally controlled analog devices that adjust the in-phase and quadrature output of an antenna at RF. One of the primary problems with the CRPA AE system is that it used analog power measurements to drive the weight adaptations; this has problems dealing with pulsed jammers, among other things. The CRPA AE system also used a crude coordinate descent algorithm in adapting the weights, which converged very slowly and sometimes exhibited erratic behavior.

The GAS-1 AE system represented a substantial improvement over the CRPA AE system. The GAS-1 AE system was partly digital; the weight updates were computed digitally using correlations measured from sampled data. However, similar to the CRPA AE system, the GAS-1 AE system employed vector modulators to adjust the weights of the auxiliary antennas at RF. Vector modulators do not allow precise control of the weight values, thereby impeding convergence and limiting null depths. In addition, the system is a null steering antenna array, and thereby has limited degrees of freedom for canceling interferers, especially since the number of antennas is only seven.

2.1.1 Shortcomings of Null Steering Antennas

A limitation of null steering antenna technology is that space-only processing requires the placing of a spatial null in the direction of each narrowband interferer as well as each wideband interferer. This leads to two problems. First, the maximum number of interferers that can be spatially nulled is $M-1$, where M is the number of antennas. Of course, given that the array aperture in the GPS application is typically on the order of a wavelength, two interferers may be relatively widely-spaced in terms of physical angle but closely-spaced in terms of beamwidths. A single null may therefore potentially take out two interferers (or more depending on their locations). **Notwithstanding,** in the GPS application, the number of antennas is small due to cost considerations, size limitations, power consumption, etc. Thus, cancellation of interferers solely through spatial nulling consumes precious degrees of freedom and thereby has limited AJ capability.

The second problem is that if an interferer and a particular GPS satellite are closely-spaced in angle, the formation of a spatial null towards that interferer may drop the gain in the direction of that GPS satellite so low that it is rendered useless. Again, due to the aforementioned small aperture problem, an interferer and GPS satellite direction may be relatively widely-spaced in terms of physical angle but closely-spaced in terms of beamwidths. In order for the GPS receiver to provide accurate navigation information, it is necessary to track the signals from at least four different GPS satellites. In order to reduce errors from various sources, it is desirable to track the respective signals from a larger number of GPS satellites. Thus, if certain types of interferers can be canceled by means other than spatial null steering, this would be highly advantageous.

2.1.2 Inherent Limitation of Power Minimization Based AJ

Again, both the CRPA AE and the GAS-1 AE system employ the principle of power minimization which attempts to drive the output power of the beamformer as close to the noise floor as possible. In so doing, nulls are only steered in the directions of those interferers whose power levels are *above* the noise floor. *This is another key shortcoming of current technology.* Smart jammers (delay spoofers, for example) can lie below the noise floor and yet totally disrupt subsequent tracking and timing calculations related to the GPS signals. The AJ schemes presented for this effort incorporate additional layers of advanced signal processing, over and above power minimization, based on the known Gold Code, for example, in order to cancel jammers below the noise floor.

This work is critical since it is expected that the number of potential military and commercial interferers will increase along with more and new jamming threats that will likely be fielded in response to the U.S. fielding of numerous GPS equipped weapon systems. Thus, innovative solutions are needed for canceling larger numbers of jammers/interferences while minimizing the impact on the GPS signal as best as possible. Fully digital solutions, ideally integrated into the GPS receiver itself, offer greater flexibility, greater accuracy, and a larger number of degrees of freedom for AJ and interference suppression.

2.2 Resulting Capability Enhancements

The AJ processors developed through this effort are capable of suppressing a mixture of interferer types including multiple broadband Gaussian noise interferers. This type of interferer is a significant threat as it is possible to distribute the jammer power across the 20.46 MHz bandwidth of the standard military P(Y) code signal centered at the GPS L1 frequency, for example, at a low enough level that it is difficult to detect and identify, and yet the noise background is increased enough to disrupt tracking of the GPS signal. This is particularly true if the enemy distributes (spatially) a number of relatively low power broadband jammers over the combat arena.

The processor also provides suppression capabilities against other types of interferers, both intentional and inadvertent. These include continuous wave (CW), swept CW, pulsed CW, phase shift keying (PSK), pseudo-noise signals (20 MHZ bandwidth), and narrowband and wideband frequency modulated signals. The interferers may be located anywhere within or adjacent to the 20.46 MHz bandwidths centered at the GPS L1 frequency of 1575.42 MHz or the L2 frequency of 1227.60 MHz, and distributed anywhere over 2π steradians of solid angle centered at zenith relative to the local horizontal plane of a GPS receiving antenna.

In addition to providing interference suppression, the processor allows reception of GPS satellite signals in a stressed environment by maximizing the signal power to interference-plus-noise power ratio (SINR) for acquisition and tracking of the GPS signal. Various user environments have been addressed. A top-down requirements study of the number of antennas and number of taps per antenna has been conducted under various user environments ranging from a foot soldier in the field, to a navy cruiser, to a high performance fighter aircraft. Various levels of integrated processing have been developed thereby offering an array of solutions that may be assessed through cost versus performance considerations.

3 Integrated AJ Processor Realizations

We have developed four different realizations of an AJ processor for GPS. The listing below is in order of increasing complexity for increased protection capability.

- *Stand-Alone Power Minimization Space-Time Preprocessor* (Section 3.3)
- *Per Satellite Power Minimization Space-Time Preprocessor* (Section 3.5)

- *Multiple Power Minimization Space-Time Preprocessors Followed by Per Satellite SINR Maximization Combining* (Section 3.6)

- *Power Minimization Space-Time Preprocessor Followed by Per Satellite MMSE Receiver Based on Known C/A Code* (Section 3.7)

The first AJ processor allows current GPS receivers to be simply retro-fitted with a front-end device. As a practical matter, though, in order to truly avoid any modification to the GPS receiver itself, the output of the space-time pre-processor must undergo D/A conversion followed by mixing back up to RF. This is obviously counter-productive when employing a digital solution but necessary in cases where a simple retro-fit is the mandated solution.

The other three AJ processors generate a different space-time filtered output for each GPS satellite in the field of view (FOV). Each of these three AJ processors may be implemented in a stand-alone fashion by summing the outputs for the different satellites and feeding the resulting sum signal to the GPS receiver. However, they are more optimally implemented as an integrated component of the overall GPS receiver wherein the space-time filtered output for the k-th GPS satellite is fed directly to the correlators and attendant timing operations matched to the k-th satellite.

Each of the three more advanced AJ processors requires an estimate of the Direction-of-Arrival (DOA) vector for the k-th GPS satellite in the FOV. The m-th element of the $M \times 1$ DOA vector for a given GPS satellite is the gain and phase of the GPS signal received from that satellite at the m-th antenna, relative to the gain and phase of the same signal at some arbitrarily chosen reference point. The DOA vector is also referred to as either the steering vector or the array manifold. In the case of an array of identical antennas, the DOA vector depends only on the azimuth and elevation angle of the GPS satellite and the locational coordinates of the antennas. In practice, though, the antennas are not identical. In fact, due to the limited aperture available, an array of diversely polarized antennas is advantageous. In addition, the limited aperture also necessitates relatively close spacing of the antennas thereby causing substantial mutual coupling effects. As a result, the DOA vector for a given GPS satellite is generally a complicated function of many parameters. Thus, a procedure for estimating the DOA vector for a given GPS satellite is presented in Section 3.4 based on the cyclostationarity of the C/A code signal.

How this DOA vector estimate is used varies amongst the three advanced AJ processors. It is initially used in beamforming to boost the Signal-to-White-Noise Ratio (SWNR) for each received GPS satellite signal by a factor equal to the number of antennas, after much of the interference has been canceled through power minimization.

3.1 Composite AJ Processor: Modular Stucture for Hierarchical AJ/Interference Cancellation

An embodiment of the fourth AJ processor has been developed that incorporates the first three AJ processors; it entails three layers of processing in a modular structure. Jammers/interferences are canceled in a hierarchical fashion. The first layer of processing entails multiple Space-Time Power Minimization (ST-PM) preprocessors as presented in Section 3.6. This first module works to cancel jammers/interferences with respective power levels *above* the noise floor. The second layer of processing is the per satellite combining of these multiple Space-Time Power Minimization (ST-PM) preprocessor outputs based on an estimate of the DOA vector. This second module works to cancel jammers/interferers with respective power levels *near* the noise floor. The third layer of processing entails a Minimum Mean Square Error (MMSE) receiver, based on the known C/A Gold Code, applied to the output of module 2. This third module works to cancel jammers/interferers with respective power levels *below* the noise floor, including delay spoofers and multipath propagation. *The ability to defeat electronic attack in the form of smart or spoofing jammer is a key feature of the composite AJ processor.*

3.2 Key Enabling Technology: Multi-Stage Nested Wiener Filter

All of the AJ processors above make use of the Multi-Stage Nested Wiener Filter (MSNWF) developed by Dr. Scott Goldstein. The MSNWF represents a pioneering breakthrough in adaptive filtering. It provides rapid convergence relative to to standard LMS based adaptations, and a dramatic reduction in computational complexity relative to standard RLS based adaptations, especially in the case of large dimension adaptive weight vectors as required for this project. *The MSNWF is a key enabling "technology" facilitating real-time implementation of the space-time adaptive algorithms for GPS AJ protection developed as part of this project.* A brief overview of the MSNWF is presented here.

Adaptive filtering schemes center upon a linear Minimum Mean Square Error (MMSE) estimation problem. In any linear MMSE problem, the optimum weight vector $\mathbf{w}$ is the solution to the Wiener-Hopf equation

$$\mathbf{R}_{xx}\mathbf{w} = \mathbf{r}_{dx} \tag{1}$$

where $\mathbf{R}_{xx}$ is the correlation matrix of the data and $\mathbf{r}_{dx}$ is the cross-correlation vector between the data and the "desired" signal. The LMS algorithm or RLS algorithm may be used to adaptively compute the solution to (1), allowing for the fact that the second order statistics actually vary with time. LMS is a stochastic gradient descent algorithm.

The RLS algorithm provides significantly faster convergence than the LMS algorithm but at a high computational cost, especially in the case of a "long" weight vector. Adaptation in a high-dimensional space implies slow convergence for both the LMS and RLS algorithms. Faster convergence can be achieved by constraining the weight vector to lie in a low-dimensional subspace. The trick is do this with little or no attendant increase in the (asymptotic) mean square error (MSE).

Prior work along the lines of dimensionality reduction restricted the weight vector $\mathbf{w}$ to lie in a subspace spanned by the Principal Components (PC) or dominant eigenvectors of $\mathbf{R}_{xx}$. Although this speeds up convergence, there is the intense computational burden of computing the dominant eigenvectors of $\mathbf{R}_{xx}$. A breakthrough occurred in 1997 when Dr. Goldstein formulated the Multi-Stage Nested Wiener Filter (MSNWF); the MSNWF was first presented at the *IEEE Military Communications Conference* in November 1997.

The MSNWF represents a pioneering breakthrough in that it simultaneously achieves a convergence speed-up substantially better than that achieved with PC **and** a dramatically reduced computational burden relative to PC as well. Intuitively speaking, achieving the best of both worlds – faster convergence AND reduced computation – is made possible by making use of the information inherently contained in both $\mathbf{R}_{xx}$ and $\mathbf{r}_{dx}$ in choosing the reduced-dimension subspace that $\mathbf{w}$ is constrained to lie within. In contrast, PC only makes use of the information embedded in $\mathbf{R}_{xx}$.

In MSNWF, there is no computation of eigenvectors. It has been shown that MSNWF implicitly constrains the weight vector to lie in the Krylov subspace spanned by $\{ \mathbf{r}_{dx}, \mathbf{R}_{xx}\mathbf{r}_{dx}, \mathbf{R}_{xx}^2\mathbf{r}_{dx}, \cdots, \mathbf{R}_{xx}^{D-1}\mathbf{r}_{dx} \}$. The word "implicit" is used since there are implementations of the MSNWF that do not require the formation of the correlation matrix. This point is addressed later.

One key, although subtle, benefit of the MSNWF is that this algorithm can work in the critical low-sample support operational environment where other adaptive algorithms fail. In other words, the ability for rapid adaptation is matched by a lower requirement for training data to estimate the statistics. Thus while many least-squares algorithms or orthogonal filter structures may offer faster convergence than stochastic gradient algorthms, the MSNWF is the only algorithm which actually reduces the sample support requirements without degrading performance. Moreover, this presents the ability to track nonstationary signal environments. Finally, it has been demonstrated that the MSNWF is extremely robust to real-world sensor effects that lead to catastrophic failure in other adaptive algorithms.

The MSNWF algorithm is summarized below. The interpretation of the "desired" signal $d_0[n]$ varies amongst the different AJ processors.

- *Initialization:* $d_0(n)$ and $\mathbf{x}_0(n) = \mathbf{x}(n)$

- *Forward Recursion:* For $k = 1, 2, ..., D$:

$$\begin{aligned} \mathbf{p}_k &= E\{d_{k-1}^*(n)\mathbf{x}_{k-1}(n)\}/||E\{d_{k-1}^*(n)\mathbf{x}_{k-1}(n)\}|| \\ d_k(n) &= \mathbf{p}_k^H \mathbf{x}_{k-1}(n) \\ \mathbf{B} &= \mathbf{I} - \mathbf{p}_k\mathbf{p}_k^H \\ \mathbf{x}_k(n) &= \mathbf{B}\mathbf{x}_{k-1}(n) \end{aligned} \tag{2}$$

- *Backward Recursion:* For $k = D, D-1, ..., 1$, with $\epsilon_D(n) = d_D(n)$:

$$\begin{aligned} w_k &= E\{d_{k-1}^*(n)\epsilon_k(n)\}/E\{|\epsilon_k(n)|^2\} \\ \epsilon_{k-1}(n) &= d_{n-1}(n) - w_k^*\epsilon_k(n) \end{aligned} \tag{3}$$

It can be easily shown that

$$\mathbf{p}_{k+1} = \frac{(\mathbf{I} - \mathbf{p}_k\mathbf{p}_k^H)\mathbf{R}_{k-1}\mathbf{p}_k}{||(\mathbf{I} - \mathbf{p}_k\mathbf{p}_k^H)\mathbf{R}_{k-1}\mathbf{p}_k||} \tag{4}$$

where

$$\mathbf{R}_{k+1} = (\mathbf{I} - \mathbf{p}_{k+1}\mathbf{p}_{k+1}^H)\mathbf{R}_k(\mathbf{I} - \mathbf{p}_{k+1}\mathbf{p}_{k+1}^H) \tag{5}$$

for $k = 0, 1, ..., D-1$, where $\mathbf{p}_1 = \mathbf{r}_{dx}$ and $\mathbf{R}_0 = \mathbf{R}_{xx}$. It follows that the matrix $\mathbf{T}_D = [\mathbf{p}_1\ \mathbf{p}_2\ ...\ \mathbf{p}_D]$ contains orthonormal columns and that the reduced dimension $D \times D$ correlation matrix $\mathbf{T}_D^H\mathbf{R}_{xx}\mathbf{T}_D$ is tri-diagonal.

The MSNWF is depicted in Figure 1 which clearly displays the multiple stages and nested structure. Operating in a D-dimensional space is tantamount to "cutting off" all stages below the D-th stage. The updating of the scalar weights ω_k in Figure 1 may be effected through a simple LMS algorithm. We have also have developed recursive adaptations for updating the so-called blocking matrices $\mathbf{B}_k$ in an RLS type fashion. The appropriate implementation of the MSNWF for each of the different AJ processors is described in the ensuing sections. The impressive capabilities of the MSNWF are demonstrated in Section 3.3.2 for the case of a space-time power minimization based preprocessor.

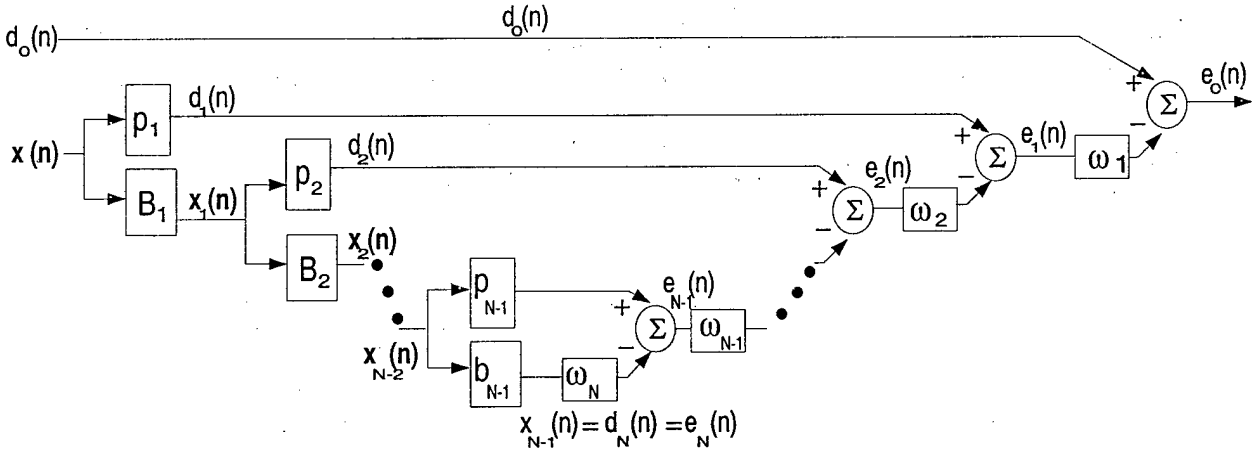

Figure 1: Structure of successive stages of the Multistage Nested Wiener Filter.

3.3 Power Minimization Based Space-Time Preprocessor

As discussed previously, the power minimization principle is based on the fact that prior to correlation, the C/A code signal from any GPS satellite is on the order of 30 dB below the noise floor. (The P code is even further below the noise floor.) A proven and widely used means of interference suppression for GPS is based on the principle of power minimization. In the case of space-only processing, the weight for the reference antenna is set to unity and the weights for the auxiliary antennas are determined as those which drive the output power of the beamformer as close to the noise floor as possible. This adaptively steers spatial nulls in the directions of those interferers whose power levels are above the noise floor.

A system based on space-only processing requires the placing of a spatial null in the direction of each narrowband interferer as well as each wideband interferer. As discussed in Section 2.1, this consumes precious degrees of freedom and potentially blots out angular sectors of space where GPS satellites lie. *Again, both CRPA AE and GAS-1N systems only allow for space-only processing.* **In contrast**, space-time processing only requires the formation of a "point-like" null in the multi-dimensional spectrum at the frequency-angle coordinates of each strong *narrowband* interferer. A sharp line null, *i.e.,* a spatial null across the entire frequency band, is still required along the angular coordinates of each broadband interferer. These nulling characteristics of power minimization based space-time pre-processing are illustrated in Figures 3(c) and 3(f), which is discussed shortly.

Since it is desirable to track the respective signals from as many GPS satellites as possible, the space-time preprocessor should "pass" unaltered as many GPS signals as possible while canceling the interference. Mathematically, it is desired that the multidimensional Fourier Transform of the space-time weights be as flat in magnitude as possible. In the case of space-time power minimization, distortion to a GPS signal from a given satellite can occur if a narrowband interferer arrives from the **same** azimith-elevation direction as that satellite. Note, though, that if one employs space-only processing to take out a narrowband interferer under these same conditions, the particular GPS satellite is taken out by the spatial null as well.

The disadvantage of space-time processing relative to space-only processing is the large dimensionality of the space-time weight vector. Referring to Figure 2, there are N taps per each of M antennas ostensibly requiring adaptation in an NM-dimensional space, as opposed to an M-dimensional space in the case of space-only processing. The higher dimensionality translates into a large computational burden and slow convergence. The MSNWF is employed to counter these deleterious effects. Illustrative preliminary simulation results are presented in Section 3.3.2 demonstrating the impressive capabilities of the MSNWF.

The primary innovation in the space-time extension of the power minimization based preprocessor, developed as part of this effort as a basic module for the more advanced AJ processors presented, is effecting it adaptively with the MSNWF. There are additional advantages over and above the speed-up in convergence and reduction in computational burden afforded by the MSNWF. For example, it allows for a larger number of "taps" per antenna (large N) without taking too much of a "hit" in terms of convergence and computational burden. This facilitates the formation of sharper spectral nulls in canceling narrowband interferers, implying less distortion to the GPS signals.

3.3.1 Formulation of Objective Function

The data is obtained by baseband I & Q frequency conversion at each antenna followed by A/D conversion at a Nyquist rate commensurate with the 20.46 MHz band occupied by the P code signal. Referring to Figure 2, $\mathbf{x}_m(n)$ is an $N \times 1$ vector containing N successive samples of the output of the m-th antenna sampled at a rate above or equal to the Nyquist rate for the P(Y) signal.

$$\mathbf{x}_m(n) = [x_m(n), x_m(n-1), ..., x_m(n-N+1)]^T, \quad m = 1, 2, ..., M. \tag{6}$$

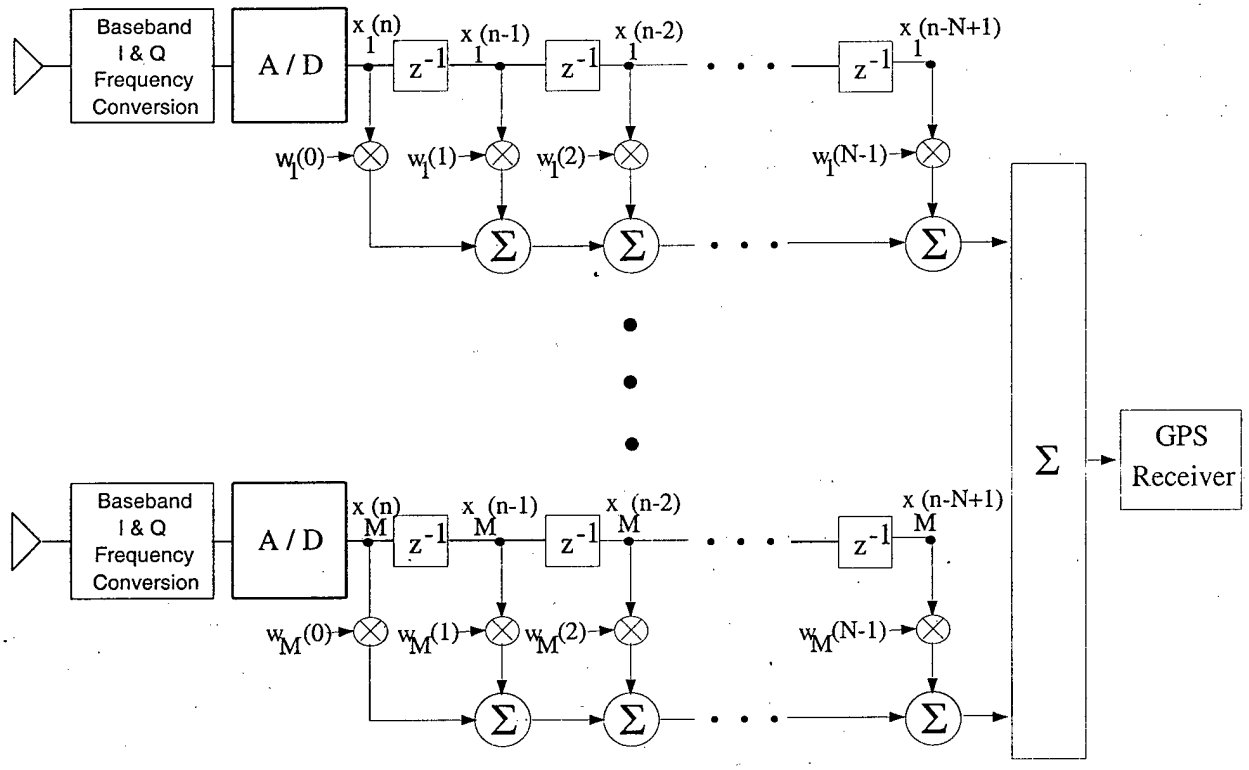

Figure 2: Adaptive filter structure for power minimization based space-time preprocessor.

Similarly, the N tap weights for the m-th antenna are placed as the components of an $N \times 1$ vector as

$$\mathbf{w}_m = [w_m(0), w_m(1), ..., w_m(N-1)]^T, \quad m = 1, 2, ..., M. \tag{7}$$

The $NM \times 1$ space-time snapshot, $\tilde{\mathbf{x}}(n)$, and the $NM \times 1$ weight vector, $\tilde{\mathbf{w}}$ are formed from concatenating $\mathbf{x}_m(n)$, $m = 1, 2, ..., M$, and $\mathbf{w}_m$, $m = 1, ..., M$, respectively, as

$$\tilde{\mathbf{x}}(n) = \begin{bmatrix} \mathbf{x}_1(n) \\ \mathbf{x}_2(n) \\ \vdots \\ \mathbf{x}_M(n) \end{bmatrix} \qquad \tilde{\mathbf{w}} = \begin{bmatrix} \mathbf{w}_1 \\ \mathbf{w}_2 \\ \vdots \\ \mathbf{w}_M \end{bmatrix}. \tag{8}$$

To incorporate the unity weight constraint on the first tap of the m-th antenna, we define $\mathbf{x}_{-m}(n)$ as the $(NM-1) \times 1$ sub-vector of $\tilde{\mathbf{x}}(n)$ containing all but the first element of $\mathbf{x}_m(n)$, $x_m(n)$. Similarly, $\mathbf{w}$ is defined as the $(NM-1) \times 1$ sub-vector of $\tilde{\mathbf{w}}$ containing all but the first element of $\mathbf{w}_m$. With these definitions, the power at the preprocessor output may be expressed as

$$\mathcal{E}\{|\tilde{\mathbf{w}}^H \tilde{\mathbf{x}}(n)|^2\} = \mathcal{E}\{|x_m(n) + \mathbf{w}^H \mathbf{x}_{-m}(n)|^2\}. \tag{9}$$

where $\mathcal{E}$ denotes expected value in a statistical sense and $(\cdot)^H$ denotes conjugate transpose. Expressing the preprocessor output power in this fashion facilitates an adaptive filtering formulation where the output of the first tap of the m-th antenna serves as the "desired" signal such that the "error" signal is $x_m(n) + \mathbf{w}^H \mathbf{x}_{-m}(n) = x_m(n) - (-\mathbf{w}^H \mathbf{x}_{-m}(n))$. This facilitates the use of LMS and/or RLS based per sample adaptations in which the "desired signal" is the output of the first tap at the m-th antenna. For the MSNWF, $d_0(n) = x_m(n)$ in Figure 1.

Jammer Type	Power	*AOA* Ex.1	*AOA* Ex.2	Bandwidth
Wideband	-100 dBW	20°	20°	20 MHz
Wideband	-110 dBW	–	0°	20 MHz
Wideband	-100 dBW	–	−20°	20 MHz
Wideband	-100 dBW	–	−40°	20 MHz
Wideband	-110 dBW	–	−60°	20 MHz
Jammer Type	SNR	*AOA*	*AOA*	Freq. relative to L1
Narrowband	-100 dBW	60°	60°	-10 MHz
Narrowband	-100 dBW	15°	–	-5 MHz
Narrowband	-100 dBW	−10°	–	0 MHz
Narrowband	-100 dBW	−30°	–	5 MHz
Narrowband	-110 dBW	−55°	–	10 MHz

Table 1: Interference parameters for illustrative simulations presented in Figure 3. Noise floor is at -127 dBW.

3.3.2 Illustrative Proof-of-Concept Simulation Examples: MSNWF Implementation of Power Minimization Space-Time Preprocessor

The illustrative proof-of-concept simulation result presented here employed $N = 7$ taps at each of $M = 7$ antenna elements equi-spaced along a line. Although typical antenna arrays for GPS are two-dimensional (planar), circular, for example, or conformal, a linear array was used in this illustrative simulation example in order to have only one angular variable for display purposes. This allows the use of a single mesh or contour plot to display the two-dimensional Fourier Transform of the space-time weights obtained from a given run.

In addition, $N = 7$ is a very small number of taps to employ at each antenna. A significantly larger number is needed in practice in order to form sharp 'point-nulls' at the angle-frequency coordinates of a narrowband interferer and thereby minimize distortion to the GPS signal. Finally, the number of jammers employed in the simulations was arbitrarily chosen to be six. The number of jammers that can be handled in practice depends on the type of jammers and varies amongst the various AJ algorithms with the more complex algorithms being able to handle a larger number of interferers. Again, the results presented here are merely preliminary proof-of-concept illustrative simulations providing evidence of the power of the MSNWF algorithm.

Table 1 summarizes the parameters of the wideband and narrowband jammers simulated in each of two different scenarios. The angles-of-arrival (AOA's) listed are relative to broadside; the frequency listed for each narrowband jammer is its offset relative to L1. The first scenario involved five narrowband jammers and one wideband jammer. The attendant results are plotted in Figure 3(a) through 3(c). The second scenario involved one narrowband jammer and five wideband jammers. The attendant results are plotted in Figure 3(d) through 3(f). In all cases, the first tap at the first antenna was constrained to be unity. Given the 20.46 MHz receiver bandwidth at each antenna, the noise floor was determined to be approximately -128 dBW. Recall the goal of power minimization is to drive the output power of the space-time beamformer as close to the noise floor as possible.

Convergence Performance. Figures 3(a) and 3(d) plot the average power output of the space-time power minimization preprocessor based on the MSNWF as a function of subspace dimension or rank of the dimensionality reducing matrix transformation. The subspace dimension at which MSNWF approximately achieves the performance of the full-dimension ideal (asymptotic) Wiener filter is roughly the same in both scenarios, around eight. In contrast, Principal Components (PC)

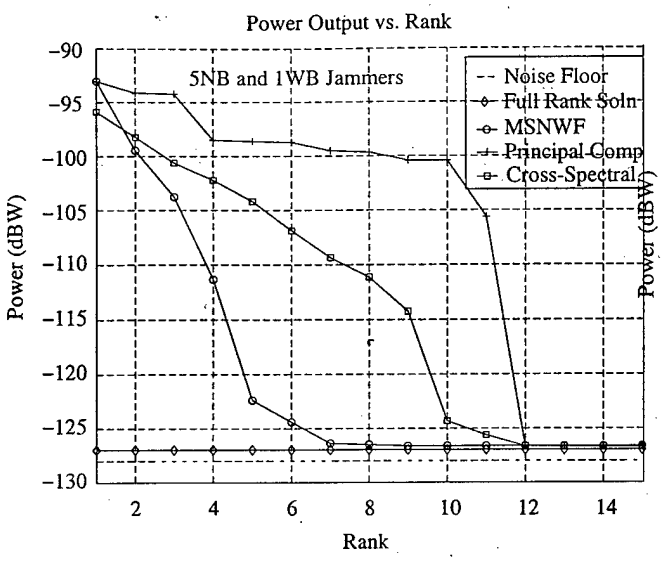

3(a). Power Output vs Rank: 1 WB, 5 NB.

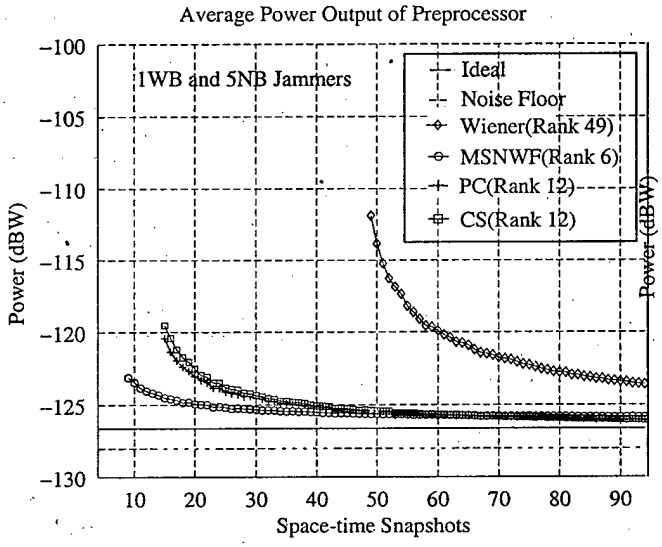

3(b). Power Output vs Snapshots: 1 WB, 5 NB.

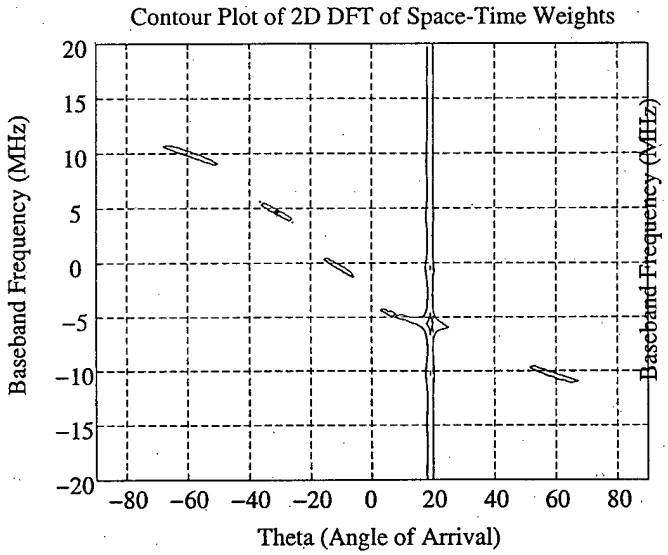

3(c). Angle-Frequency Response: 1 WB, 5 NB.

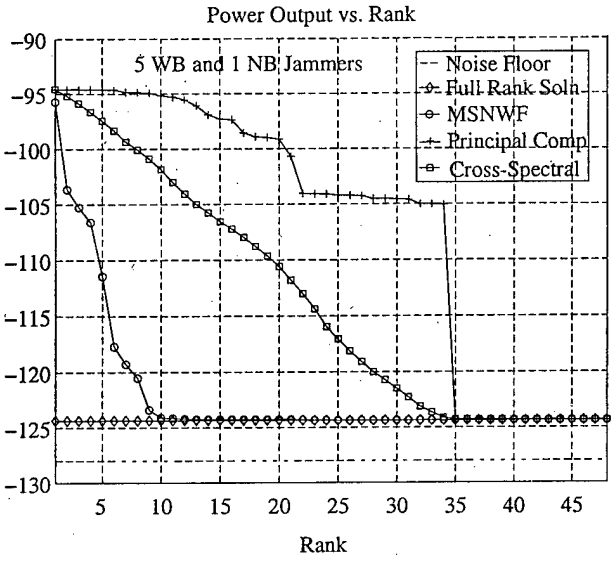

3(d). Power Output vs Rank: 5 WB, 1 NB.

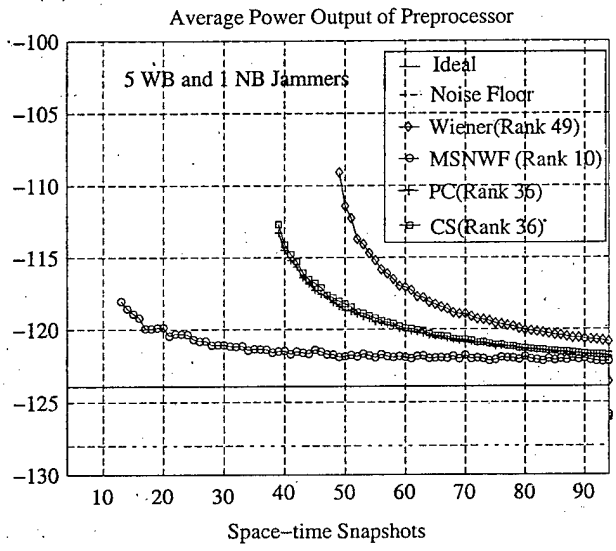

3(e). Power Output vs Snapshots: 5 WB, 1 NB.

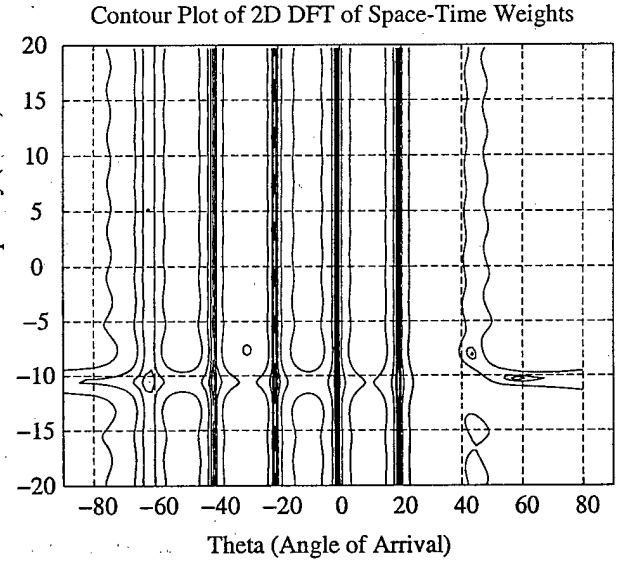

3(f). Angle-Frequency Response: 5 WB, 1 NB.

generally requires a subspace dimension equal to the number of degrees of freedom taken up by the jammers to achieve the same output power level. Each narrowband jammer takes up one degree of freedom. Each wideband jammer takes up $N = 7$ degrees of freedom, where N is the number of taps per antenna. This is because the cancellation of a wideband jammer requires a spatial null, implying a null across the entire 20.46 MHz spectrum at its AOA. In Scenario 1, the jammers take up $5 \times 1 + 1 \times 7 = 12$ degrees of freedom; in Scenario 2, the jammers take up $1 \times 1 + 5 \times 7 = 36$ degrees of freedom.

Figures 3(b) and 3(e) examine the space-time snapshot sample support necessary to effectively null the jammers for each of the two scenarios simulated. The power output for each sample support level was averaged over 250 Monte Carlo trial runs. The greatest differential in performance between the MSNWF and PC based methods is observed in Figure 3(e) corresponding to Scenario 2. In this case, Figure 3(d) and the above calculation dictate that PC needs to adapt in a 36-dimensional subspace, while the MSNWF need only adapt in a 10-dimensional space. This allows MSNWF to converge more rapidly than PC.

Computational Performance. At the same time, there is no computation of eigenvectors involved in the MSNWF. Only a small number of simple matrix-vector multiplications are needed to determine the required low-dimensional subspace. In contrast, the computation of the 36 eigenvectors needed by the PC method in Scenario 2 is a substantial computational burden. Note, though, that PC does indeed converge more quickly than the full-dimension (49), finite-sample Wiener filter. Note that Figure 3 also displays the performance of the Cross-Spectral Metric (CSM) method. Similar to the PC method, the CSM method constrains the space-time weight vector to lie in a subspace spanned by a subset of the eigenvectors of the space-time correlation matrix. The choice of eigenvectors is dictated by a cross-spectral metric derived from the cross-correlation vector, rather than simply choosing those eigenvectors associated with the largest eigenvalues. CSM yields improved performance relative to PC, but its performance is not nearly as good as MSNWF and it too requires the computation of eigenvectors.

Nulling Performance/Distortion Issues. Figures 3(c) and 3(f) display contour plots of the magnitude of the multi-dimensional Fourier Transform of the space-time weights obtained from the MSNWF with 40 space-time snapshots. For Scenario 1, Figure 3(c) displays a well-defined "point-null" at the angle-frequency coordinate of each narrowband jammer and a well-defined "line-null" along the arrival angle of the wideband jammer. For Scenario 2, Figure 3(f) displays a well-defined "point-null" at the angle-frequency coordinate of the one narrowband jammer and a well-defined "line-null" along the respective arrival angle of each of the five the wideband jammers. As important, in both cases the response of the space-time beamformer is observed to be relatively flat away from the null locations.

3.4 DOA Vector Estimation Based on Cyclostationarity of C/A Code Signal

The other three AJ processors developed as part of this effort produce a different space-time filtered output for each GPS satellite in the FOV. A key component of each of these three AJ processors is exploitation of the cyclostationarity of the C/A code signal to estimate the Direction-of-Arrival (DOA) vector for a given GPS satellite. Again, the m-th element of the $M \times 1$ DOA vector for a given GPS satellite is the gain and phase of the GPS signal received from that satellite at the m-th antenna, relative to the gain and phase of the same signal at some arbitrarily chosen reference point. *Exploitation of cyclostationarity enables one to estimate the DOA vector for a GPS satellite* **even in the presence of strong interference from multiple sources.**

How this DOA vector estimate is used varies amongst the different methods. It is initially used in beamforming to boost the Signal-to-White-Noise Ratio (SWNR) for each received GPS satellite signal by a factor equal to the number of antennas, after much of the interference has been canceled through power minimization. This is discussed shortly.

The DOA vector obtained by processing the C/A code signal may be used advantageously in processing the P code signal from that same satellite since the two signals arrive from the same

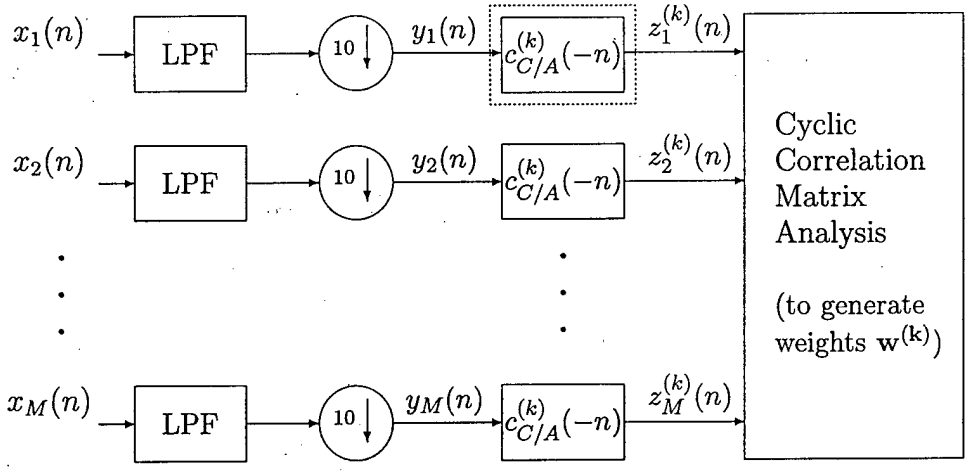

Figure 5: Cyclostationarity based method for estimating the DOA vector for the k-th GPS satellite in the field of view. As a result of Doppler effects, the block shown within a dashed box (and each of the other same blocks) is implemented via a bank of parallel filters effecting partial despreading as shown in in Figure 6.

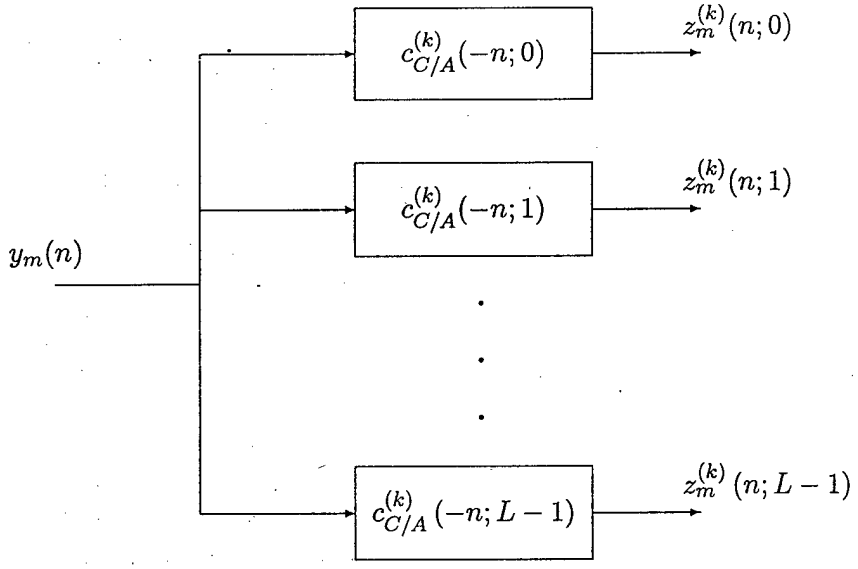

Figure 6: Partial despreading via a bank of L parallel filters derived as length Q (nonoverlapping) sub-blocks of the 1023 length Gold Code for the k-th GPS satellite.

direction. This is discussed later. The C/A code signal is used to find the DOA vector for a given GPS satellite since it is cyclostationary, arising from the fact that the same 1023 length Gold Code is repeated every millisecond. The P code signal is cyclostationary but on a much, much longer time scale.

3.4.1 Partial Despreading Due to Doppler Shift Effects

Estimation of the DOA vector for a given GPS satellite is facilitated by boosting its SWNR and its SINR as much as possible, prior to cyclic spatial correlation matrix analysis (to be explained shortly). To this end, we first perform digital lowpass filtering at each antenna, as indicated in Figure 5, since the C/A code signal only occupies one-tenth of the bandwidth occupied by the P code signal. Accordingly, the filtered signal at each antenna may be decimated or downsampled by a factor of ten to produce the outputs, $y_m(n)$, $m = 1, ..., M$. The combination of the lowpass filtering and decimation has been efficiently implemented through multirate DSP using polyphase filters.

Ideally, this would be followed by correlating and summing with the C/A code for the k-th GPS satellite in the FOV, sliding over one chip (over one half-chip with two times per chip sampling of C/A signal) at a time. As indicated in Figure 5, continual correlation in this fashion is equivalent to running each output $y_m(n)$ through a filter whose impulse response is the time-reverse of the C/A code. Since the C/A code is repeated twenty times in one bit of navigation information, an additional 13 dB boost in SWNR could be achieved by continuous correlation with a sequence formed from twenty repetitions of the C/A code for the k-th satellite. However, the signal arriving from each GPS satellite may be Doppler shifted as much as up to $\pm$ 5 KHz away from L1 (or L2) due to motion of the satellite, thereby effectively destroying the processing gain.

In fact, the Doppler shifts are potentially large enough that the variation in phase over just one Gold Code block is substantial. Now, the cyclostationarity based method for estimating the DOA vector is immune to Doppler effects as a result of both an inherent magnitude squaring and the fact that the Doppler shift for a given GPS satellite is the same at each receive antenna. However, its efficacy depends on the SWNR of the satellite signal of interest being "boosted" above other signals that repeat at the same rate.

This is where the **partial despreading** is used. The idea is to break the length 1023 Gold Code for a given GPS satellite into L nonoverlapping sub-blocks of length Q. The ℓ-th sub-block of the k-th Gold Code $c^{(k)}(n)$ is denoted $c^{(k)}(n;\ell)$. Q is chosen as large as possible under the constraint that the change in phase over the sub-block due to Doppler be small enough to achieve a processing gain for each sub-block as close to Q as possible. Since interfering signals that do not repeat at the same rate as the C/A code asymptotically have vanishing contribution to the cyclic spatial correlation matrix (to be mathematically defined shortly), a processing gain of 18 dB is more than sufficient for the purpose of estimating the DOA vector for the k-th satellite via the cyclostationarity scheme presented in the next section.

In the trade-off between processing gain and Doppler effects, a reasonable possibility for starters is to decompose the Gold Code into $L = 16$ blocks of length $Q = 64$. For the sake of notational simplicity, the last block is padded with a single zero. Optimal designs have been developed though performance analysis.

Thus, as depicted in Figure 6, the outputs $y_m(n)$ are then passed through a bank of L parallel filters where the impulse response of the ℓ-th filter is the time-reverse of the ℓ-th sub-block of the Gold Code associated with the k-th GPS satellite, denoted $c^{(k)}(n;\ell)$. This creates the outputs $z_m^{(k)}(n;\ell)$, where m is the antenna index, k is the satellite index and ℓ is the sub-block index.

3.4.2 Cyclic Correlation Matrix Analysis

The above process yields a "finger" in the ℓ-th sub-block output at the m-th antenna every 1023 samples, multiplied by both a navigation information bit value and the m-th value of the DOA vector.

At this point, the relative locations of the fingers are unknown and they may not be detectable due to interference despite the 18 dB processing gain. For the ℓ-th sub-block, we thus propose to form the following cyclic spatial correlation matrix of dimension equal to the number of antennas, M.

$$\mathbf{R}_{zz}^{\alpha}(\ell) = \frac{1}{N_s} \sum_{n=0}^{N_s-1} e^{-j2\pi \frac{n}{1023}} \mathbf{z}^{(k)}(n;\ell)\mathbf{z}^{(k)H}(n;\ell) \tag{10}$$

where $\mathbf{z}^{(k)}(n) = [z_1^{(k)}(n;\ell), z_2^{(k)}(n;\ell) z_M^{(k)}(n;\ell)]^T$ and N_s is the number of C/A code blocks over which $\mathbf{R}_{zz}^{\alpha}(\ell)$ is averaged. *Note that the time duration over which $\bar{\mathbf{R}}^{\alpha}$ is averaged may span numerous cycles of the Doppler shift modulation since the asymptotic structure of $\bar{\mathbf{R}}^{\alpha}$ is not affected by Doppler.* The immunity of $\bar{\mathbf{R}}^{\alpha}$ to Doppler effects is a result of both the magnitude squaring inherent in the conjugate transpose operation denoted by H and the fact that the Doppler shift is the same at each receive antenna.

In the asymptotic limit, $\mathbf{R}_{zz}^{\alpha}(\ell)$ only has contributions from signals that have the same cycle frequency, repeat every 1023 samples. Any jammer that does not repeat at this rate will asymptotically have vanishing contribution to $\mathbf{R}_{zz}^{\alpha}(\ell)$, as does the noise. In the case of no delay spoofers, we have shown that the dominant contribution to $\mathbf{R}^{\alpha}(\ell)$ is proportional to $e^{-j2\pi \frac{\tau_k + \ell Q}{1023}} \mathbf{a}^{(k)}\mathbf{a}^{(k)H}$, where $\mathbf{a}^{(k)}$ is the DOA vector for the k-th GPS satellite and τ_k is the relative time location of the "finger" in the first sub-block code filter output, relative to a single period of the C/A code spanning 1023 chips. The phase factor $e^{j2\pi\ell\frac{Q}{1023}}$ accounts for the fact that the "fingers" occurring in the ℓ-th sub-block output are offset in time by ℓQ units relative to the "fingers" occurring in the first sub-block output, $l = 0, 1, ..., L-1$.

Two methods for averaging the L values of $\mathbf{R}_{zz}^{\alpha}(\ell)$ have been investigated. First, they may be incoherently averaged as

$$\bar{\mathbf{R}}_{incoherent}^{\alpha} = \frac{1}{L} \sum_{\ell=0}^{L-1} \mathbf{R}_{zz}^{\alpha}(\ell)\mathbf{R}_{zz}^{\alpha H}(\ell) \tag{11}$$

Recall that the dominant contribution to $\mathbf{R}^{\alpha}(\ell)$ is proportional to $e^{-j2\pi \frac{\tau_k + \ell Q}{1023}} \mathbf{a}^{(k)}\mathbf{a}^{(k)H}$, which is not Hermitian-symmetric. Second, the L values of $\mathbf{R}_{zz}^{\alpha}(\ell)$ may be coherently averaged as

$$\bar{\mathbf{R}}_{zz}^{\alpha} = \frac{1}{L} \sum_{\ell=0}^{L-1} \lambda^{\ell} e^{j2\pi\ell\frac{Q}{1023}} \mathbf{R}_{zz}^{\alpha}(\ell). \tag{12}$$

The weighting λ is ideally of the form $e^{-j\Delta}$, where Δ is the center phase offset of one sub-block relative to the next due to the Doppler modulation. Procedures for estimating λ to elevate the contribution of the desired satellite signal, over and above the 18 dB processing gain achieved with partial despreading with sub-blocks of length $Q = 64$, have been developed as part of this project.

Note that Section 3.6 proposes applying this DOA estimation procedure at the output of a bank of parallel ST-PM preprocessors, as shown in Figure 9, where interferers above the noise floor are already canceled. In this case, only jammers below the noise floor that repeat at this rate will potentially contribute significantly to $\bar{\mathbf{R}}_{zz}^{\alpha}$. Given that the contribution from the k-th GPS satellite benefits from an 18 dB processing gain, the only types of jammers that will contribute significantly to $\bar{\mathbf{R}}_{zz}^{\alpha}$ are delay spoofers.

In the case of no delay spoofers, the dominant contribution to $\bar{\mathbf{R}}^{\alpha}$ is proportional to $\mathbf{a}^{(k)}\mathbf{a}^{(k)H}$, Thus, a couple of power iterations may be employed to estimate the dominant left singular vector of $\bar{\mathbf{R}}^{\alpha}$ and thereby provide an estimate of the DOA vector $\mathbf{a}^{(k)}$ (to within an unknown multiplicative scalar inconsequential for beamforming purposes).

If there are J delay spoofers, $\bar{\mathbf{R}}_{zz}^{\alpha}$ will be of the form

$$\mathbf{R}_{zz}^{\alpha} = e^{-j2\pi \frac{\tau_k}{1023}} \mathbf{a}^{(k)}\mathbf{a}^{(k)H} + \sum_{p=1}^{J} e^{-j2\pi \frac{\tau_q}{1023}} \mathbf{a}^{(p)}\mathbf{a}^{(p)H} \tag{13}$$

where $\mathbf{a}^{(p)}$ is the DOA vector for the q-th delay spoofer and τ_p is its corresponding relative time delay. Methods for canceling delay spoofers are presented shortly.

3.4.3 Proof-of-Concept Experiment: Cyclostationarity Based Interference Cancellation

The efficacy of exploiting the cyclostationarity of the C/A code signal to estimate the DOA vector for a given GPS satellite and ultimately combat interference is demonstrated using data derived from an experimental test-bed built at the Polytechnic University of Madrid through a collaboration between Dr. Zoltowski and the Electromagnetics Group there. A brief description of the test-bed is provided below.

A block diagram is shown in Figure 7 (a). The antenna array consists of 6 elements equi-spaced along a circle of radius equal to roughly half-wavelength at L1. Each antenna element is a low cost *stacked patch antenna*. This configuration provides a wide bandwidth allowing the reception of INMARSAT as well as GPS. To achieve circular polarization, a 90° hybrid is placed below each element. (A picture of the experimental prototype in Figure 8 (a) shows the physical antenna array structure.) Following this are six Low Noise Amplifiers (LNA) in MMIC. The RF outputs of the six antennas are handed to six standard DS-SS receivers with the special feature that all of them are locked to the same Local Oscillator (LO). These six spread spectrum receivers are basically composed of two stages: downconversion from RF to IF, followed by digital down conversion from IF to BaseBand (BB). Only the C/A code signal was processed in this prototype.

An experiment was conducted in which the experimental GPS receiver was programmed to receive a GPS signal arriving at an elevation angle of 30 degrees with respect to the boresite axis of the array. After despreading, the SNR of the GPS signal was roughly 10 dB per element. In addition, interference was intentionally injected by a nearby radiating antenna at an angle of 20 degrees with respect to boresite, and at a power level 40 dB above the desired GPS signal (prior to despreading). A 6×6 cyclic spatial correlation matrix, $\mathbf{R}_{zz}^{\alpha}$, was formed from the outputs of each antenna in the manner described previously. In addition, a standard spatial correlation matrix was formed as $\mathbf{R}_{zz} = \frac{1}{N_s} \sum_{n=0}^{N_s-1} \mathbf{z}^{(k)}(n)\mathbf{z}^{(k)H}(n)$. The interferer did not have the same cycle frequency as the C/A code. Therefore, $\mathbf{R}_{zz}^{\alpha}$ essentially had one dominant term proportional to $\mathbf{a}^{(k)}\mathbf{a}^{(k)H}$. The standard correlation matrix was approximately of the form $\mathbf{R}_{zz} = \sigma_k \mathbf{a}^{(k)}\mathbf{a}^{(k)H} + \sigma_p \mathbf{a}^{(p)}\mathbf{a}^{(p)H} + \sigma_w \mathbf{I}$, where σ_k, σ_ℓ, and σ_w reflect the relative power levels of the jammer, the GPS signal (post-correlation), and the receiver noise, respectively. $\mathbf{a}^{(p)}$ is the DOA vector for the interferer.

Rather than compute an estimate of the GPS DOA vector $\mathbf{a}^{(k)}$ from the largest left singular vector of $\mathbf{R}_{zz}^{\alpha}$ (since the array was not well-calibrated), a set of beamforming weights was determined by computing the largest generalized eigenvector of the matrix pencil $\{\mathbf{R}_{zz}^{\alpha}, \mathbf{R}_{zz}\}$. In order to give some idea of the improvement achieved, in Figure 7 (c) the eye diagram at the antenna element with the best SNR is compared with that obtained at the beamformer output. It is clear that the jammer has been sufficiently rejected so as to "open up the eye."

A very important aspect of exploiting cyclostationarity is that it steers the beam and adapts the nulls based only on the known C/A code. Due to nonlinear effects amongst the individual antennas, the most predominant of which arise from mutual coupling, it is difficult and expensive to design antenna arrays calibrated well enough to achieve beamforming through phase shifts derived from the azimuth and elevation coordinates of a given GPS satellite and the locations of the antennas.

3.5 Per Satellite Power Minimization Space-Time Preprocessor

The Space-Time Power Minimization (ST-PM) based preprocessor does NOT yield maximal SINR for any GPS satellite, but rather attempts to "pass" all GPS satellite signals in the FOV as undistorted as possible while canceling the interference. Two shortcomings of the ST-PM based preprocessor are (1) it does not attempt to minimize distortion to any one GPS satellite signal and (2) it does not take advantage of the SWNR gain possible through co-phasal beamforming for a given GPS satellite.

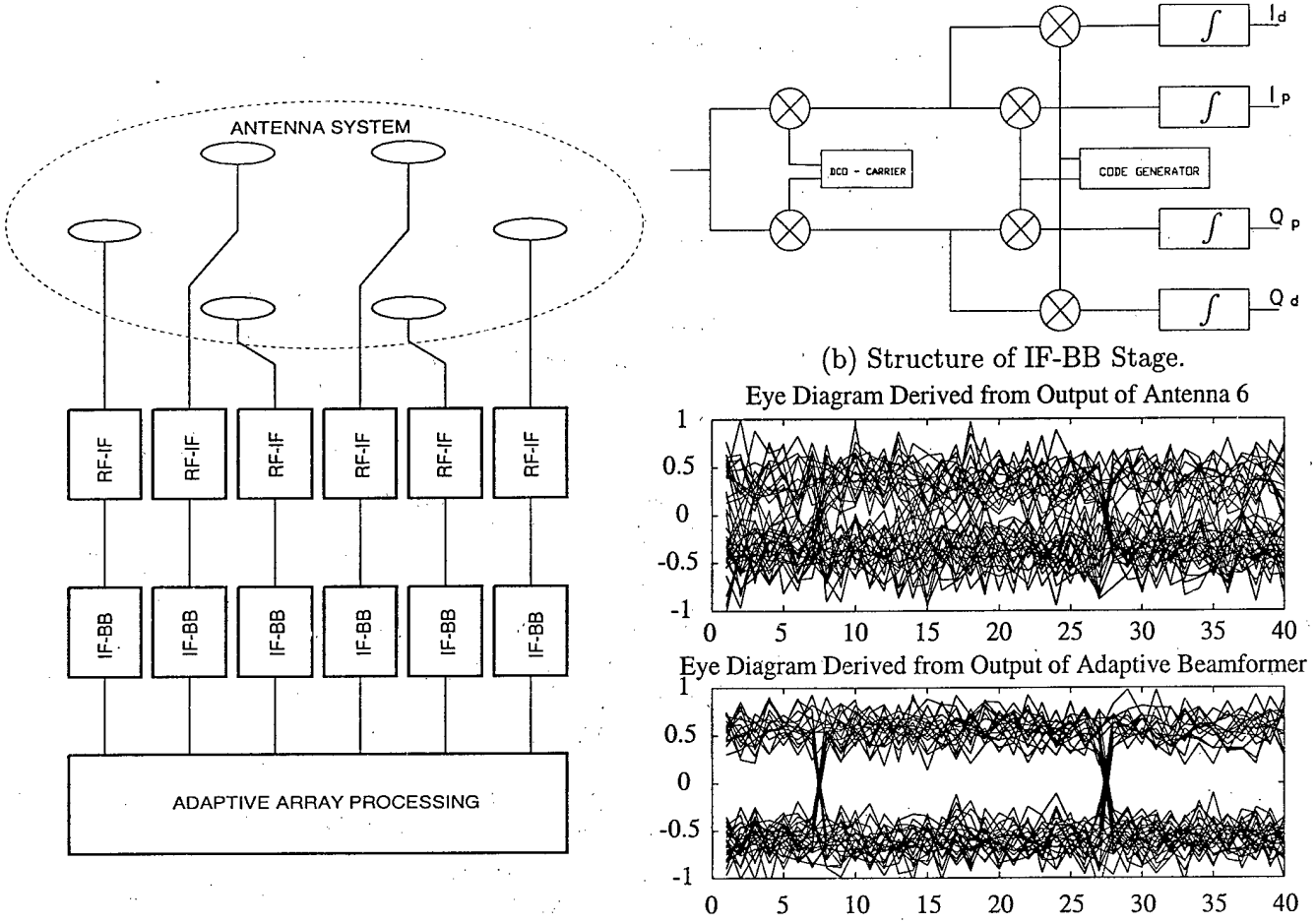

(a) Block diagram of prototype/test-bed. (b) Structure of IF-BB Stage. (c) Eye diagrams from experimental data.

Figure 7: Experimental prototype developed at the Polytechnic University of Madrid in collaboration with Purdue University.

It is presented that the estimate of the DOA vector for a given GPS satellite, $\hat{\mathbf{a}}_k$, obtained via the presented cyclostationarity based scheme, be used to achieve these goals as follows.

First, a different ST-PM preprocessor is needed for each of the K GPS satellites in the FOV. Thus, achieving the above two goals to enhance GPS protection comes at a significant computational cost. Efficient implementation of the K parallel constrained ST-PM preprocessors using the MSNWF have been developed as part of this project. Since a different space-time weight vector is formed for each satellite, this is denoted by placing a superscript k on the weight vector $\mathbf{w}$.

For the k-th satellite, we constrain the inner product between $\hat{\mathbf{a}}_k$ and the $M \times 1$ vector of weights associated with the **same** time instant but spanning the M antennas, $\tilde{\mathbf{w}}_n^{(k)} = [w_1^{(k)}(n), w_2^{(k)}(n), ..., w_M^{(k)}(n)]^T$, to be unity for each of the N "tap times" comprising the space-time adaptive filter structure. This leads to power minimization with N linear constraints:

$$\underset{\mathbf{w}}{\text{Minimize}} \quad \mathbf{w}^{(k)H}\mathbf{R}_{xx}\mathbf{w}^{(k)} \tag{14}$$

$$\text{Subject to: } \mathbf{w}^{(k)H}\mathbf{T}_n\hat{\mathbf{a}}_k = 1, \;\; n = 0, 1, ..., N-1$$

where $\mathbf{T}_n$ is a selection matrix composed of ones and zeroes such that $\tilde{\mathbf{w}}_n^{(k)} = \mathbf{T}_n^T\mathbf{w}^{(k)}$, where $\tilde{\mathbf{w}}_n^{(k)} = [w_1^{(k)}(n), w_2^{(k)}(n), ..., w_M^{(k)}(n)]^T$, as defined above. Accommodating the N linear constraints consumes

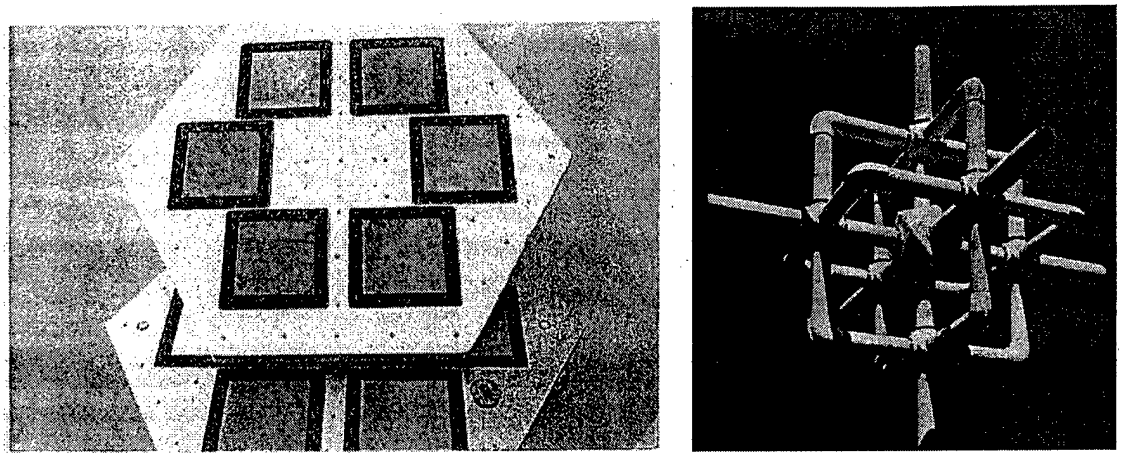

(a) Prototype stacked patch antenna array. (b) Compact array for DF at HF.

Figure 8: Examples of experimental compact arrays with polarization diversity.

N out of NM degrees of freedom. Implementations of the MSNWF that accommodate multiple linear constraints have been developed as part of this project.

Again, a different constrained ST-PM filtered output is created for each satellite in the FOV. If a retro-fit is required to existing GPS UE, the outputs obtained by doing this for each of the K satellites in the FOV may be simply summed and fed to the GPS receiver (after D/A and frequency conversion back to L1). This is suboptimal as well as inefficient. If the AJ functions were integrated into the GPS receiver and operated synergistically with its standard functions, the 1-D signal created for the k-th GPS satellite created by this method would be sent directly to a code-tracker (and Doppler tracker) matched to that satellite.

3.6 Multiple Power Minimization Space-Time Preprocessors and Per Satellite Combining

Although the procedure in Section 3.4 for estimating the DOA vector for the k-th satellite is effective even in the presence of strong interference, it may require averaging over many bits before the interference contribution to the cyclic correlation matrix is small enough to obtain a reliable estimate of $\mathbf{a}^{(k)}$. We thus propose a methodology for canceling as much interference as possible before estimating the DOA vector. The architecture presented for such may be used as the first stage of a multi-stage AJ process, where the first stage attempts to cancel jammers above the noise floor. This facilitates cancellation of other AJ waveforms hovering at or below the noise floor in subsequent stages as discussed in Section 3.7.

The key idea is to create M different ST-PM preprocessors as shown in Figure 9: the m-th one is created by constraining the weight value for the *first* tap at the m-th antenna to be unity; the remaining space-time weights are chosen as those which yield minimum output power. Efficient implementations of the M parallel ST-PM preprocessors using the MSNWF have been developed.

This yields M linearly independent ST-PM outputs as shown in Figure 9. In each case, interferers above the noise floor are ideally canceled. The *magnitude* of the angle-frequency spectrum of the m-th set of space-time weights is relatively smooth with point nulls at the angle-frequency coordinates of each narrowband jammer, and a line null in frequency at the angle of each broadband jammer. *The idea is to use the estimated DOA vector for the k-th GPS satellite to combine the M ST-PM outputs so that the response of the angle-frequency spectrum of the composite sum of weighted ST-PM preprocessors, the m-th one weighted by $\alpha_m^{(k)}$ as shown in Figure 9, is* elevated *along the angular direction of that satellite, i.e., so that its SWNR is ideally boosted by a factor of M.* This is achieved through co-phasal beamforming where $\alpha_m^{(k)}$ is equal to the complex conjugate of the DOA vector associated with the k-th

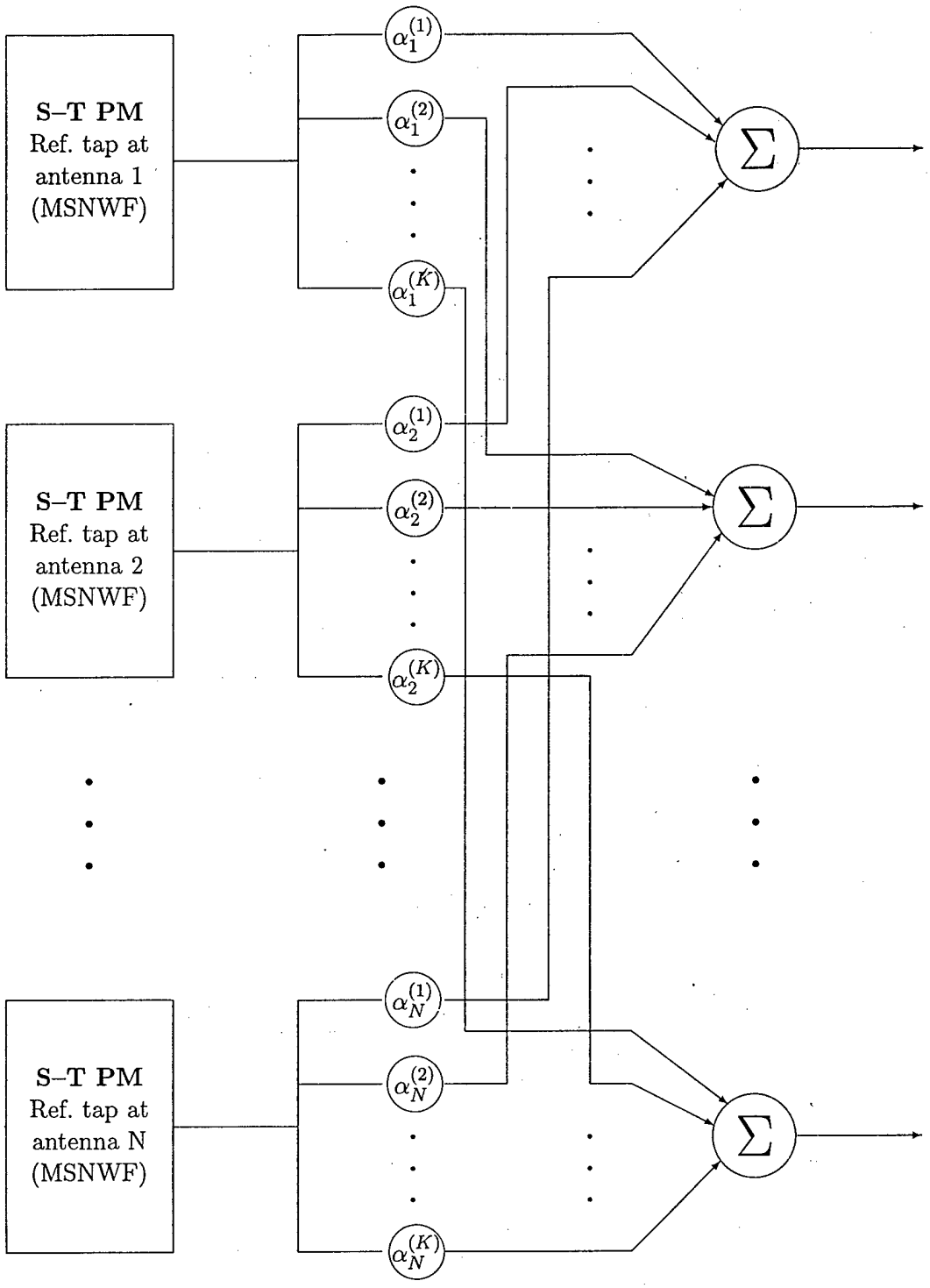

Figure 9: Multiple Space-Time Power Minimization (ST-PM) Preprocessors.

GPS satellite.

The M different ST-PM weights transform the data from the original M-dimensional element-space to an M-dimensional *reduced interference* beamspace. The DOA vector for each satellite will generally be altered through this transformation process. It is thus necessary to apply the cyclostationarity based DOA vector estimation module in Figure 5 at the outputs of the M ST-PM preprocessors. In fact, it is highly advantageous to do this since the interference is substantially reduced at the outputs of the M ST-PM preprocessors. Combined with the processing gain achieved by correlating and summing with sub-blocks of the C/A code for the k-th satellite, the reduction in interference causes the "largest" left singular vector of the $M \times M$ cyclic correlation matrix to converge quickly to the DOA vector in the M-dimensional *reduced interference* beamspace data.

Now, a preprocessor based on the power minimization principle can only cancel jammers/interferers above the noise floor. Smart jammers can lie at or below the noise floor and still disrupt subsequent tracking and timing calculations related to the GPS signals. Thus, rather than do simple co-phasal beamforming with the DOA vector estimate $\hat{\mathbf{a}}^{(k)}$, added interference protection may be achieved by doing adaptive beamforming at the outputs of the M ST-PM preprocessors.

To this end, let $\hat{\mathbf{R}}_{xx}$ be an $M \times M$ spatial correlation matrix (not cyclic) formed at the outputs of the M ST-PM preprocessors (in the M-dimensional *reduced interference* beamspace). What we propose is to use the MSNWF to solve the system of equations $\hat{\mathbf{R}}_{xx}\boldsymbol{\alpha}^{(k)} = \hat{\mathbf{a}}^{(k)}$. Weighting and summing the M ST-PM outputs with the elements of $\boldsymbol{\alpha}^{(k)}$ thus computed, as shown in Figure 9, represents a per satellite combining that works to suppress jammers/interferers at or just below the noise floor while maintaining an SWNR gain of M as best as possible.

3.7 Power Minimization Space-Time Preprocessor Followed by Per Satellite MMSE Receiver Based on Known C/A Code

As discussed in Section 3.1, the fourth AJ processor presented incorporates the second and third presented AJ processors as the first two layers of processing, and adds a third layer of processing. The first layer of processing entails multiple Space-Time Power Minimization (ST-PM) preprocessors as presented in Section refSTPMBank, working to cancel jammers/interferences *above* the noise floor. The second layer of processing is the per satellite combining of these multiple Space-Time Power Minimization (ST-PM) preprocessor outputs based on an estimate of the DOA vector. This works to cancel jammers/interferers *near* the noise floor. The third layer of processing entails a Minimum Mean Square Error (MMSE) receiver applied to the output of module 2 based on the known C/A Gold Code. This works to cancel jammers/interferers with respective power levels *below* the noise floor, including delay spoofers and multipath propagation.

The presented MMSE receiver works in code-space to effect cancellation of multi-user access interference (MAI) in direct-sequence spread spectrum (DS-SS) systems where the code for each user is repeated for each and every transmitted information symbol, as is the case for the C/A code signal. The key concepts underlying the algorithm are explained in terms of how it would be applied in the case of the C/A code signal. Let $\mathbf{c}^{(k)}$ denote an $N_G \times 1$ vector containing the $N_G = 1023$ length Gold Code for the k-th GPS satellite. Let $B_0^{(k)}$ denote an $N_G \times (N_G - 1)$ blocking matrix containing as columns $N_G - 1$ vectors, each of which is orthogonal to $\mathbf{c}^{(k)}$. Each column of $B_0^{(k)}$ is viewed as an FIR (digital) filter as is $\mathbf{c}^{(k)}$.

Once synchronization with the GPS from the k-th satellite is achieved, each of the respective outputs of the bank of $N_G - 1$ parallel filters formed from the columns of $B_0^{(k)}$ only contains interference or jammers, assuming one slides over a full Gold Code duration at a time. A weighted sum of these is thus used to estimate the interference contaminating the output of the code-matched filter $\mathbf{c}^{(k)}$. The receiver adapts the weighting of the respective outputs of the $N_G - 1$ parallel filters formed from the columns of $B_0^{(k)}$ so as to minimize the mean square value of the difference between the resulting sum and the output of $\mathbf{c}^{(k)}$.

3.7.1 Combining Partial Despreading and the Multi-Stage Nested Wiener Filter: A Powerful Innovation

The weight vector to be adapted is essentially as long as the code length. In order to speed up convergence, and to reduce computational complexity, We have applied the MSNWF to this problem by defining the "desired" signal as the output of the the code-matched filter $\mathbf{c}^{(k)}$. This yielded a reduced-rank adaptive algorithm for finding that weight vector which maximizes the post-correlation SINR for a given "user" knowing only the code of that "user", the C/A code in our application here. This prior work primarily deals with commercial CDMA systems, where the channel code length is on the order of a 100. Here the Gold Code lenth is 1023, an order of magnitude higher. Ostensibly, this translates into a very large computational burden.

However, as pointed out in Section 3.4.1, there are relatively large Doppler shifts due to satellite motion. *Thus, to reduce the computational complexity* **AND** *counter the deleterious effects of Doppler, we propose to once again employ the method of partial despreading.* The length 1023 Gold Code for a given GPS satellite is decomposed into L nonoverlapping sub-blocks of length Q, with Q chosen as large as possible under the constraint that the change in phase over the sub-block due to Doppler be relatively negligible. Since Q can still be quite large, $L = 16$ blocks of length $Q = 64$ is a reasonable starting point, we propose to apply the MSNWF to the output of each sub-block. This combination of partial despreading and the MSNWF is a truly powerful innovation that has not heretofore been developed for any CDMA application.

3.8 Polarization Diverse Arrays and Compact Arrays

As noted previously, the formation of a spatial null towards an interferer may drop the gain in the direction of a "nearby" (in angle) GPS satellite so low that it is rendered useless. Due to the small array aperture in the GPS application, an interferer and a GPS satellite may be widely-spaced in terms of physical angle but closely-spaced in terms of beamwidths. Polarization diversity amongst the antenna elements is a way to combat this problem.

For example, consider the compact array pictured in Figure 8 (b) used for direction finding (DF) and beamforming at HF for electronic warfare applications. This compact array consists of three orthogonal loops and three orthogonal dipoles, all co-located but having mutually orthogonal orientations. Dr. Zoltowski has developed algorithms for DF and beamforming which exploit the polarization diversity inherent in this compact array [Zo6, Zo7]. For example, it has been demonstrated that two signals coming from exactly the same radial direction but with different polarization states may be extracted individually!

Again, though, the compact array pictured in Figure 8 (b) was developed for operation at HF. It was presented here solely for the purpose of emphasizing the importance of polarization diversity. For the GPS application, effecting polarization diversity amongst the antenna elements may be as simple as having adjacent antenna elements oppositely polarized, clock-wise circular followed by counter clock-wise circular in sequence. Compact nonlinear antenna arrays and alternative realizations of polarization diversity have been investigated as part of this project.

In the GPS application, the beamforming weights that yield maximum SINR for a given GPS satellite have a complex dependence on on the polarization states and azimuth/elevation angles of both that satellite's signal and the interfering signals. This dependence is further complicated by mutual coupling effects. However, all of the algorithms presented for this project adapt either based on the power minimization principle or the the known code of a given GPS satellite. The optimal weights are achieved automatically without the need for estimating polarization states or azimuth/elevation angles.

4 PERSONNEL SUPPORTED

Faculty:	Michael D. Zoltowski (PI)
Graduate Students:	Wilbur Myrick
	Anand Kannan

5 PUBLICATIONS

5.1 Journal Papers Published and/or Accepted

1. K. T. Wong and M. D. Zoltowski, "ESPRIT-Based Direction Finding Using A Sparse Rectangular Array with Dual-Size Spatial Invariances," *IEEE Transactions on Aerospace and Electronic Systems,* October 1998, pp. 1320-1336.

2. J. Ramos, C. P. Mathews, and M. D. Zoltowski, "Closed-Form 2D Angle Estimation Algorithms for Filled Circular Arrays with Arbitrary Sampling Lattices," *IEEE Trans. on Signal Processing,* vol. 47, no. 1, Jan. 1999, pp. 213-217.

3. John Shynk and Michael D. Zoltowski, "Blind Adaptive Beamforming for Cellular Communications," **Highlights of Signal Processing for Communications**), *IEEE Signal Processing Magazine*, March 1999, pp. 27-31.

4. K. T. Wong and M. D. Zoltowski, "Root-MUSIC Based Azimuth-Elevation Angle-of-Arrival Estimation for Uniformly-Spaced but Arbitrarily Oriented Velocity Hydrophones," *IEEE Transactions on Signal Processing,* vol. 47, no. 12, December 1999, pp. 1350-1360.

5. J. Ramos, M. D. Zoltowski, and Hui Liu, "Low-Complexity Space-Time Processor for DS-CDMA Communications," *IEEE Trans. on Signal Processing,* vol. 48, no. 1, January 2000, pp. 39-52.

6. K. T. Wong and M. D. Zoltowski, "Self-Initiating MUSIC-Based Direction Finding in Underwater Acoustic Particle Velocity-Field Beamspace," *IEEE Journal of Oceanic Engineering,* vol. 25, no. 2, pp. 262-273, April 2000.

7. Yung-Fang Chen, M. D. Zoltowski, J. Ramos, C. Chatterjee, and V. Roychowdhury, "Reduced Dimension Blind Space-Time RAKE Receivers for DS-CDMA Communication Systems," *IEEE Trans. on Signal Processing,* vol. 48, no. 6, June 2000, pp. 1521-1536.

8. Yung-Fang Chen and M. D. Zoltowski, "Blind RLS Based Space-Time Adaptive 2D RAKE Receivers for DS-CDMA Communication Systems," *IEEE Trans. on Signal Processing,* vol. 48, no. 7, July 2000, pp. 2145-2149.

9. M. D. Zoltowski and K. T. Wong, "ESPRIT-Based 2D Direction Finding with a Sparse Uniform Array of Electromagnetic Vector-Sensors," *IEEE Transactions on Signal Processing,* vol. 48, no. 8, August 2000, pp. 2205-2210.

10. K. T. Wong and M. D. Zoltowski, "Closed-Form Eigenstructure-Based Direction Finding Using Arbitrary but Identical Subarrays on a Sparse Uniform Rectangular Array Grid," *IEEE Transactions on Signal Processing,* vol. 48, no. 8, August 2000, pp. 2195-2204.

11. K. T. Wong and M. D. Zoltowski, "Closed-Form Direction Finding & Polarization Estimation with Arbitrarily-Spaced Electromagnetic Vector Sensors at Unknown Locations," *IEEE Transactions on Antennas and Propagation,* vol. 48, no. 5, May 2000, pp. 671-681.

12. T. Krauss and M. D. Zoltowski, "Multiuser Second-Order Statistics Based Blind Channel Identification for Using a Linear Parameterization of the Channel Matrix," *IEEE Trans. on Signal Processing,* vol. 48, no. 9, September 2000, pp. 2473-2486.

13. K. T. Wong and M. D. Zoltowski, "Self-Initiating MUSIC Based Direction Finding in Polarized Beamspace," accepted for publication in *IEEE Transactions on Antennas and Propagation,* acceptance letter dated 11 February 1999, **Scheduled for August 2000.**

5.2 Conference Papers Published and/or Accepted

1. Yung-Fang Chen and M. D. Zoltowski, "Blind 2-D RAKE Receivers Based on RLS-Type Space-Time Adaptive Filtering for DS-CDMA System," *Proc. of 1998 IEEE Int'l Conf. on Acoustics, Speech, and Signal Processing,* 12-15 May 1998, Seattle, WA.

2. K. T. Wong and M. D. Zoltowski, "Closed-Form Direction-Finding with Arbitrarily Spaced Electromagnetic Vector-Sensors at Unknown Locations," *Proc. of the 1998 IEEE Int'l Conf. on Acoustics, Speech, and Signal Processing,* 12-15 May 1998, Seattle, WA.

3. Yung-Fang Chen and Michael D. Zoltowski, "Convergence analysis and tracking capability of reduced dimension blind space-time RAKE receivers," *IEEE Vehicular Technology Conference (VTC) '98,* Ottawa, Ontario, Canada, 18-21 May 1998, pp. 2333-2337.

4. T. Krauss and M. D. Zoltowski, "Zero Forcing Equalization of Multiple FIR Channels Via Oversampling," *invited paper Eighth IEEE Digital Signal Processing Workshop,* Bryce Canyon National Park, Utah, 9-12 August 1998.

5. M. D. Zoltowski and A. Kannan, "Rotational Signature Blind Co-Channel Signal Separation," *Eighth IEEE Digital Signal Processing Workshop,* Bryce Canyon National Park, Utah, 9-12 August 1998.

6. Yung-Fang Chen and Michael D. Zoltowski, "Joint angle and delay estimation for reduced dimension space-time RAKE receiver with application to IS-95 CDMA uplink," *IEEE Fifth International Symposium on Spread Spectrum Techniques and Applications (ISSSTA) '98,* Sun City, South Africa, volume 2, pp. 606-610, 2-4 Sept. 1998.

7. M. D. Zoltowski and Der-Feng Tseng, "A Weighted Energy Concentration Criterion for Improving the Performance of Deterministic Least Squares Blind Channel Identification," *Proceedings of 1998 IEEE Midwest Symposium on Circuits and Systems MWSCS '98,* University of Notre Dame, 9-12 August 1998, pp. 148-152.

8. T. F. Settle, M. D. Zoltowski, and V. Balakrishnan, "Design of Multichannel Equalizers Via Linear Matrix Inequalities: Trade-Offs Between SNR and ISI," *Proc. of the 1998 IEEE Workshop on Statistical Signal and Array Processing, SSAP '98,* September 1998, Portland, OR.

9. M. D. Zoltowski and Der-Feng Tseng, "Blind Multichannel Equalization for Wideband TDMA Based on Subbanding and the SIMO Cross-Relation," (invited paper) *Proceedings 36th Annual Allerton Conference on Communications, Systems, and Computing,* 23 Sept.- 25 Sept. 1998, pp. 381-390.

10. M. D. Zoltowski and Der-Feng Tseng, "Blind Multichannel Identification for High-Speed TDMA," (invited paper) *Proceedings of Milcom '98,* Boston, MA, 18-21 Oct. 1998. **Winner of "The Fred Ellersick MILCOM Award for Best Paper in the Unclassified Technical Program".**

11. M. D. Zoltowski and D. Tseng, "A Weighted Energy Concentration Criterion for Improving the Performance of the Cross-Relation Method of Blind Channel Identification at Low SNR" *invited paper, Conf. Record of the 32nd Asilomar IEEE Conference on Signals, Systems, and Computers,* pp. 785-789, 30 Oct.-1 Nov. 1998.

12. M. D. Zoltowski and T. A. Thomas, "Novel Zero-Forcing, MMSE, and DFE Equalizer Structures Employing Oversampling and Multiple Receiver Antennas," *invited paper, Conf. Record of the 32nd Asilomar IEEE Conference on Signals, Systems, and Computers,* pp. 1111-1116, 30 Oct.-1 Nov. 1998.

13. Yung-Fang Chen and M. D. Zoltowski, "Joint Angle and Delay Estimation for DS-CDMA With Application to Reduced Dimension Space-Time Rake Receivers," *Proc. of 1999 IEEE Int'l Conf. on Acoustics, Speech, and Signal Processing,* Phoenix, Arizona, 15-19 March 1999.

14. Thomas P. Krauss and M. D. Zoltowski, "Multiuser Blind Identification Using a Linear Parameterization of the Channel Matrix and Second-Order Statistics," *Proc. of 1999 IEEE Int'l Conf. on Acoustics, Speech, and Signal Processing*, Phoenix, Arizona, 15-19 March 1999.

15. M. D. Zoltowski and Der-Feng Tseng, "A Subbanding Approach to Blind Space-Time Equalization for Wideband TDMA Based on the SIMO Cross-Relation," *SPIE's International Symposium on AeroSense,* Orlando, Florida, **SPIE Proceedings Volume 3708: Digital Wireless Communications**, pp. 20-33, 5-9 April 1999.

16. M. D. Zoltowski and Der-Feng Tseng, "A Filter Bank Approach to Blind Space-Time Equalization for Wideband TDMA," *Proceedings of IEEE Vehicular Technology Conference (VTC) '99,*, Houston, TX, 17-21 May 1999.

17. Anand Kannan and M. D. Zoltowski, "Resynchronization of Co-channel Narrowband Digital Signals," *2nd IEEE Signal Processing Advance in Wireless Communications Workshop - SPAWC '99,* Annapolis, Maryland, pp. 138-141, 9-12 May 1999.

18. Wilbur Myrick, M. D. Zoltowski and J. Scott Goldstein, "Smoothing of Space-Time Power Minimization Based Preprocessor for GPS," (Invited paper). *Second joint USA/Australia Workshop in Defense Applications of Signal Processing (DASP99),* Chicago, IL, Starved Rock State Park, 22-26 August 1999, pp.125-130.

19. W. Myrick, M. D. Zoltowski, J. S. Goldstein, "Interference Suppression for CDMA via a Space-Time Power Minimization Based Preprocessor with Applications to GPS," *Proceedings 37th Annual Allerton Conference on Communications, Systems, and Computing,* 23-24 Sept. 1999, pp. 196-203.

20. M. D. Zoltowski and Thomas P. Krauss, "Space-Time Zero Forcing Equalization for 3G CDMA Forward Link to Restore Orthogonality of OVSF Channel Codes," (invited paper) *Proceedings 37th Annual Allerton Conference on Communications, Systems, and Computing,* 23-24 Sept. 1999, pp. 1274-1283

21. Wilbur Myrick, M. D. Zoltowski and J. Scott Goldstein, "Anti-Jam Space-Time Preprocessor for GPS Based on Multistage Nested Wiener Filter," *IEEE Military Communications (Milcom '99),* Atlantic City, NJ, 3-6 Oct. 1999.

22. Thomas P. Krauss and Michael D. Zoltowski, "Blind Channel Identification on CDMA Forward Link Based on Dual Antenna Receiver at Hand-set and Cross-Relation," *invited paper, Conf. Record of the 33rd Asilomar IEEE Conference on Signals, Systems, and Computers,* 25-27 Oct. 1999.

23. Thomas P. Krauss, Michael D. Zoltowski, and Samina Chowdhury, "Two-Channel Zero Forcing Equalization on CDMA Forward Link: Trade-Offs Between Multi-User Access Interference and Diversity Gains," *invited paper, Conf. Record of the 33rd Asilomar IEEE Conference on Signals, Systems, and Computers,* 25-27 Oct. 1999.

24. Wilbur Myrick and M. D. Zoltowski, "GPS Jammer Suppression with Low-Sample Support Using Reduced-Rank Power Minimization," *Proc. of the 10th IEEE Workshop on Statistical Signal and Array Processing, SSAP 2000,* Pocono Manor, PA, 14-16 August 2000, pp. 514-518.

25. Wilbur Myrick and Michael D. Zoltowski, "Low-Sample Performance of Reduced-Rank Power Minimization Based Jammer Suppression for GPS," *IEEE Sixth International Symposium on Spread Spectrum Techniques & Applications (ISSSTA 2000)*, Parsippany, NJ, 6-8 September 2000, pp. 93-97.

26. W.L. Myrick, M.D. Zoltowski, and J.S. Goldstein, "Adaptive Anti-Jam Reduced-Rank Space-Time Preprocessor Algorithms for GPS," *Institute of Navigation (ION) Conference,* Salt Lake City, Utah, 17-20 Sept. 2000.

6 INTERACTIONS/TRANSITIONS:

6.1 A. Participation/presentations at meetings, conferences, seminars, etc

6.1.1 Invited Seminars.

- "Space-Time Signal Processing for Wireless Communications: Equalization and Interference Cancellation," ECE Dept. Colloquium at University of Minnesota (televised), *(invited by Prof. Ahmed Tewfik)* 12 February 1998.

- "Smart Antennas for Wireless Communications," *(invited by Prof. Mani Venkata)* Jerry Junkins Endowed Chair Seminar Series, Department of Electrical and Computer Engineering, Iowa State University, Ames, IA, 13 February 1996.

- "Semi-Blind Space-Time Equalization for High-Speed Linear/Nonlinear Modulations Based on Subbanding and the SIMO Cross-Relation" *(invited by Dr. Timothy Thomas)* Communications Systems Research Lab, Motorola, Schaumburg, IL, 18 December 1998.

- "Overview of Physical Layer Standards and Related Space-Time Signal Processing Research at Purdue University for Third Generation Wireless Communications," ECE Dept. Colloquium at University of Virginia (Eminent Speaker Series), *(invited by Prof. Nikos Siridopolous)* 12 May 1999.

- "Overview of Physical Layer Standards and Related Space-Time Signal Processing Research at Purdue University for Third Generation Wireless Communications," ECE Dept. Colloquium at University of Illinois at Chicago, *(invited by Prof. Arye Nehorai)*, 2 June 1999.

- "Dual-Channel Zero Forcing Equalization for 3G CDMA Forward Link to Restore Orthogonality of OVSF Channel Codes," NCE Cullimore Memoral Distinguished Lecture Series at New Jersey Institute of Technology, Newark, NJ, *(invited by Prof. Yeshkel Bar-Ness)*, 1 November 1999.

- "Space-Time RAKE Receiver/Zero Forcing Equalizer Hybrids for 3G CDMA Forward Link Exploiting Orthogonality of OVSF Channel Codes," ECE Dept. Colloquium at Nothwestern University, Evanston, IL, *(invited by Prof. Michael Honig)*, 12 November 1999.

6.2 B. Consultative and advisory functions to other laboratories and agencies, especially Air Force and other DoD laboratories

- Served on review panel for National Science Foundation's Wireless Information Technology and Networks Proposal Review Panel, CISE Directorate, CCR, Signal Processing Systems Program, Arlington, VA, 21-22 June 1999.

6.3 C. Transitions

None to report at this time. We will continue our dialogue with Dr. James Tsui at Wright Laboratories on the Wright-Patterson Air Force Base in Dayton, OH to work towards a transition of this research. Dr. Tsui is currently overseeing the development of an experimental multichannel receiver for GPS at Wright Labs. The initial goal of this interaction is to test the GPS anti-jam algorithms developed through this effort with experimental data supplied by Dr. Tsui. We will also continue our dialogue with Eddie Gibbs at Eglin Air Force Base to effect transitions of this research as well. We are also working to effect transitions to the GPS JPO Office through SAIC's GPS group in Los Angeles.

7 NEW DISCOVERIES, INVENTIONS, OR PATENT DISCLOSURES

No patent disclosures to report. New discoveries and inventions summarized previously.

8 HONORS/AWARDS

- Recipient along with Der-Feng Tseng of "The Fred Ellersick MILCOM Award for Best Paper in the Unclassified Technical Program" at the *IEEE Military Communications (MILCOM '98) Conference* held in Bedford, MA 19-21 October 1998. The paper was entitled "Blind Multichannel Identification for High-Speed TDMA" and the plaque was awarded by the IEEE Communications Society and the MILCOM Conference Board at the Chairman's Banquet held during the conference. I was the lead and primary author of the paper and the presenter as well. MILCOM '98 is a major IEEE sponsored conference in Communications and there was only one Paper Award out of roughly 230 unclassified papers.

- I was elected *Fellow of IEEE*, effective 1 January 1999 for "Contributions to the theory of antenna array signal processing and two-dimensional direction-of-arrival estimation". Photo and Fellow citation to be included in April 1999 issue of *IEEE Communications Magazine.*

- I was elected Secretary of the IEEE Signal Processing Society, elected 16 May 1998 by the Board of Governors, for a three year term starting 1 January 1999. As Secretary, I automatically became a member of the Executive Committee of IEEE Signal Processing Society.

- I was elected to membership in Signal Processing for Communications Technical Committee (SSAP TC) of the IEEE Signal Processing Society, elected for a three year term starting 1 January 1999.

- I continued to serve as an elected Member-at-Large of the Board of Governors of the IEEE Signal Processing Society. My three year term from 1 January 1998 and ends 31 December 2000.